Influence of laboratory aging and asphaltene content of asphalt on frictional coefficient by tribological analysis – a case study

Corentin Verilhac, Gilles Barreto, Lise Devès, Frédéric Delfosse, Stéphane Carlotti, Thomas Lebarbé, Jean-François Le-Meins

Influence of laboratory aging and asphaltene content of asphalt on frictional coefficient by tribological analysis - a case study

Corentin Verilhac[1,2,3]*, Gilles Barreto[2], Lise Devès[2], Frédéric Delfosse[3], Stéphane Carlotti[1], Thomas Lebarbé[3]*, Jean-François Le-Meins[1]

[1]Univ. Bordeaux, CNRS, Bordeaux INP, LCPO, UMR 5629, F-33600, Pessac, France
[2]Research Center Rhône-Alpes, ARKEMA, B.P. 63 Pierre-Bénite, Pierre-Bénite Cedex, France
[3]Vinci construction, Research Center, 22 rue Thierry Sabine, PO Box 20067-33703, Merignac Cedex, France

* Corresponding authors
Thomas Lebarbé: thomas.lebarbe@vinci-construction.com
Corentin Verilhac: corentin.verilhac@vinci-construction.com

Abstract:

An increase in use of reclaimed asphalt pavement (RAP) materials was observed for the last few years. These materials are composed of aged asphalt which can cause implementation issues due to its high viscosity. This work suggests a new way to explain a part of this problematic by tribological analysis and to assess the lubricating ability of aged asphalt. The influence of asphalt aging is investigated on the frictional properties using two 35/50 asphalt penetration graded specimens and a third one extracted from RAP. Short and long-term as well as natural effects of aging are examined on penetration grade, ring and ball temperature, infrared indices, and asphaltene content to demonstrate a physical hardening of the studied asphalts. The influence of natural or thermal aging are also studied by tribological measurements on lubricating properties. A ball on a three-plate equipment are used to evaluate the coefficient of friction (CoF) as a function of sliding velocity (Stribeck Curve) from 120°C to 80°C. The increase in asphaltene content after oxidation increases the frictional coefficient in the hydrodynamic regime. These observations were confirmed by tribological analysis performed on

asphalts with controlled asphaltene contents (0, 15, 20wt%). In addition of the physical hardening, asphalt oxidation causes a decrease of the lubricant properties. The evaluation of frictional coefficient can be added to the other well-known parameters to explain workability issues in presence of aged materials.

Keywords:

Asphalt, Aging, Tribology, Asphaltene, Coefficient of Friction

1 Introduction:

Nowadays, with environmental issues, reclaimed asphalt pavement (RAP) is increasingly used as raw materials for new asphalt concrete formulations[1]. Workability issues are now of strong interest and a better understanding of the asphalt present in the RAP is required.

Asphalt materials are generally described as complex mixtures of different hydrocarbons with a polarity gradient in Saturate, Aromatic, Resin and Asphaltene (SARA) fractions[2,3], which can be viewed as a colloidal suspension[4,5]. Understanding the aging of these materials is a keypoint for future developments concerning the addition of reclaimed asphalt pavement to asphalt concrete. Laboratory asphalt aging was extensively described in literature[6–10]. The natural aging of the asphalt binders is simulated using two thermal tests. The first one is the rolling thin-film oven test (RTFOT) for short-term aging[11]. This experiment attempts to generate the same hardening and physico-chemical behavior modifications as after the mixing process for the hot-mix asphalt. The aim of the second experiment, referred to as the Pressure-Aging Vessel (PAV)[12], is designed to represent the long-term aging of binders after long-term in-service roads. After these treatments, the asphalt binders are also analyzed using infrared spectroscopy to evaluate the degree of oxidation using carbonyl and sulfoxide indices[6,9]. These parameters are generally used to quantify asphalt aging and correlate with physico-chemical properties such as viscosity and viscoelastic properties[7,8].

The oxidation of asphalt is generally described in the literature by different physical and chemical modifications. Regarding the chemical aspect, oxidation can be followed by studying S=O and C=O bonds by FTIR measurements[7,10], and information can be gained also measuring SARA fraction which varying with oxidation degree[13]. This variation of SARA fraction was mainly due to the oxidation of sulfur and carbon to sulfoxide and carbonyl[14]. These heteroatoms were in principle in aromatic and resin fractions. This oxidation generates new kind of polar molecules in asphalt which are called oxidized asphaltenes. These chemical changes are generally induced by thermal oxidation. More complex reactions occur with ultraviolets radiation, as it was listed by N. C. L. Madeira and col. [6].

These chemical modifications have an influence on mechanical behavior of asphalt resulting in an increase of the storage modulus (G') and viscosity parameters. Moreover, it increases the ring and ball temperature (RBT) and decreases penetration grade. The loss of workability and mechanical properties when reclaimed asphalt materials are used in asphalt concrete formulations is generally induced by an asphalt evolution after oxidation. In some cases, these parameters were not sufficient to explain the workability and compaction properties. Tribological analysis are expected to explain some aspects of these physical behaviors.

Tribology science is used to observe the lubricant power of oil for engineering pieces[15]. Stribeck worked principally on friction phenomena present in steel balls bearing and established the so-used Stribeck curve. M. Woydt described historical events related to discovery dealing with tribological science and tell that Thuston was the first to develop an accurate system to measure the Coefficient of Friction (CoF) in 1870s[15]. Tribological experiments are used to compare different compounds based on their ability to decrease the CoF between two contact layers. In many cases, lubricants exhibit different behaviors, as identified by Stribeck. Many different tests exist to evaluate frictional parameters under different movements and conditions[16]. The first thin film analysis of asphalt were conducted by G.L. Baumgardner and col.[17,18] using a classic rheometer. Subsequently, the ball on a three-plate system is most commonly used[19–29] and the use of four-ball apparatus analysis is occasionally mentioned[23,29]; however, these experiments require more material and temperature homogenization requires more time. It is interesting to note that the use of tribology to study asphalt binders increased in the last decade[16,22,29,30].

With respect to asphalt applications, recent studies have shown that viscosity, and gyratory shear press workability on asphalt concrete[31,32] could be correlated to the minimal CoF, measured by tribology, and that the influence of chemical additives could be evaluated.

This study proposes the first evaluation of the influence of asphalt aging on the frictional properties.

2 Materials and methods:

General asphalt characterization

Characterizations were performed on different asphalt samples before and after aging based on two 35/50 1/10mm penetration graded specimens arbitrarily called Asphalt A and B with relatively similar physical-chemical properties. Those characterizations include the asphaltene content with an internal method describe afterwards in "Asphaltene extraction" part, ring and ball temperature [NF EN 1427][33], needle penetration [NF EN 1426][34], aging index by Infra-Red (IR) spectroscopy, and rheological tests. The results are summarized in Table 1. The ring and ball temperature measurement follows the standard procedure with calibrating rings and balls. A bath of water was used to vary the temperature (in °C) and a laser was used to precisely determine the softening point of the asphalt sample. Needle penetration was measured using a calibrated needle with a weight of 100 g for 5 s at 25°C.

Infrared Data treatment

Aging indices were calculated by the integration of the signals at different wavenumbers and estimated using the C-H strain peak as a reference peak (IR spectra are shown in Figures S1 and S2). The oxidation indices were calculated from the area under the peak, using the limits described in Table S1. The carbonyl index (I_{CO}) and sulfoxide index (I_{SO}) were calculated using the equations S1 and S2.

Rheological Analysis

To respect the "natural cooling" and erase the potential thermal history of asphalt, the two following rheological protocols began from higher to lower temperatures. All experiments were performed under inert atmosphere (N_2) except for Brookfield rotational viscosimeter experiments.

Rheological analysis was performed using an Anton Paar rotational controlled stress rheometer (MCR 302) to evaluate the viscosity of each asphalt specimen. Isothermal analyses, from 120°C to 80°C (increments of 10°C), were performed at a constant shear rate (=1s^{-1}) with a gap equal to 1 mm and a 25 mm plate-plate geometry. The sample was maintained at the analysis temperature for 10 min to

obtain a homogeneous sample temperature, and acquisition was performed for 10 min to ensure that the temperature did not evolve during the test. The average viscosity was then calculated and plotted as a function of the temperature (Figure S3).

Viscosity of asphalt A and B were also evaluated using a Brookfield viscometer with a coaxial cylinder's geometry in a temperature range from 180 to 60°C and following the standard NF EN 13302[35]. Two different cylinder diameters (SC4-21 and SC4-27) were used to adapt the measurement to viscosity evolution with decreasing temperature. For each measurement, the sample was maintained at the analysis temperature for 10 min and the viscosity value was collected with a value of torque at 90% of the maximum value that can be detected by the viscometer. The viscosity is plotted as a function of temperature (Figure S4).

Asphaltene / maltene extraction protocol

The asphaltenes were extracted from the asphalt binder *via* filtration. First, 1 g of asphalt binder was dissolved in 30 mL of N-heptane during 24 h. Then a filtration was carried out using a Büchner system with a PTFE filter with a porosity of 45µm to isolate the asphaltenes aggregates/particles from the filtrate solution constituted of a mixture of maltene and N-heptane. This solution was placed under vacuum to remove the N-heptane (Figure S5).

The first step was repeated with the asphaltene extract at 70°C for 2 h to wash the high-melting crystallizable fraction. Retentate asphaltene particles were collected and the filtrate was eliminated. The collected asphaltene was weighted to determine the asphaltene content in the asphalt using equation [S3].

This extraction protocol was performed on all samples and was used to control the quantity of asphaltene in the reference and aged specimens.

Laboratory aging of asphalt sample

Asphalts A and B from different origins were used and subjected to thermal aging treatment. The first concerns short-term aging using the Rolling Thin-Film Oven Test (RTFOT) process following the EN 12607-1 standard[11]. To proceed, 35 g of asphalt was added to each vial and placed in an RTFOT machine for 1h15 min at 163°C under oxidative flux at atmospheric pressure. This treatment simulates the aging process that occurs during the mixing process. The second method involved a Pressure Aging Vessel (PAV, long-term aging) following the EN 14769 standard[12]. This process was realized with 50 g of asphalt in each plate with an oxidation time of 40h at 100°C after one RTFOT and under 21 bars of oxidative flux.

Asphaltene control process for model asphalt specimen

Asphaltenes and maltenes were added to the asphalt mixture to obtain modified asphalt with controlled asphaltene content. Asphalt A has a natural content of 20.3 wt%, and asphalt B has 11.4 wt% asphaltenes. The maltene extract from asphalt A was reused to decrease the asphaltene content by dilution and obtain 15.0 wt% asphaltenes. Similarly, the asphaltene extract from asphalt B was added to increase the asphaltene content to obtain asphalt B with 15.0 wt% asphaltene. All the compounds (maltene and asphaltenes) were mixed by mechanical stirring for 5 min after heating the asphalt to 150°C for 30 min under Nitrogen atmosphere to avoid oxidation.

Asphalt extraction from Reclaimed Asphalt Pavement (RAP)

This process consists of solubilizing asphalt from RAP with a perchloroethylene solvent and following the NF EN 12697-1 standard[36]. RAP (1 kg) was added to the engine, mixed with the solvent, and centrifuged to extract the filler particles. A mixture of asphalt solubilized in a solvent was collected and placed in a rotavapor to extract the solvent. The amount of residual solvent determined by Infrared spectroscopy was negligible (<0,4%).

Finally, ten different asphalts were obtained and evaluated through tribological analysis (Table 1).

Table 1: Asphaltene content, Ring and ball temperature, needle penetration, oxidative index and viscosity at 135°C of asphalts A and B before and after RTFOT, after RTFOT + PAV 40h, at 15wt% of asphaltene, maltene A and asphalt from RAP

Asphalt origin	Name	Asphaltene content (%) [+/- 1%]	Ring and Ball Temperature (°C) [+/- 1°C]	Needle Penetration (1/10 mm) [+/- 2 dmm]	Index I_{CO} (a.u.)	Index I_{SO} (a.u.)	Viscosity at 135°C (Pa.s)	
Asphalt A	[1]AA_{REF}	20.3	52.6	50	1.1	10.8	0,842	+/- 0,039
	[2]AA_{RTFOT}	22.4	58.0	28	0.6	13.0	1,107	+/- 0,042
	[3]$AA_{RTFOTPAV}$	29.8	73.8	15	6.7	19.2	3,043	+/- 0,045
	[4]AA_{15}	15	---	---	---	---	---	---
	[5]AA_{0}	0	---	---	---	---	---	---
Asphalt B	[1]AB_{REF}	11.4	52.4	38	1.2	11.1	0,727	+/- 0,045
	[2]AB_{RTFOT}	12.9	59.0	29	1.7	11.8	1,032	+/- 0,045
	[3]$AB_{RTFOTPAV}$	25.6	70.6	16	7.5	18.5	2,283	+/- 0,043
	[4]AB_{15}	15.0	---	---	---	---	---	---
Naturally aged asphalt extract from RAP	[6]A_{RAP}	29.0	72.2	12	8.0	22.6	4,375	+/- 0,374
Standard	---	Internal Method	NF EN 1427	NF EN 1426	Internal Method		Internal Method	
Measurement | Sample number	---	1 | 2	1 | 2	3 | 1	1 | 1		1 | 1	

[1]Reference asphalt without modification,
[2]Asphalt obtained after Rolling Thin Film Oven Test oxidation time 1 hours 15 minutes at 163°C,
[3]Asphalt obtained after RTFOT and Pressure Aging Vessel during 40 hours at 100°C,
[4]Asphalt obtained after modification by addition of maltene or asphaltene to get a modified asphalt at 15 wt% of asphaltene,
[5]Maltene obtained after the internal method for asphaltene extraction by N-heptane at room temperature (first extraction step),
[6]Asphalt extract by Infratest protocol from reclaimed asphalt pavement.

Tribological analysis

Tribological analysis was performed with an Anton Paar rotational controlled stress Rheometer MCR 302 with three-plates ball system as shown in Figure S6.

Stainless steel plates were used and handled with nitril gloves for all the following experiments and washed with technical ethanol and acetone to remove every trace of grease which can influence the experimental values. The experimental conditions were the same as in the work of Ingrassia L. *et.al.*[27] (except for the sliding velocity ramp) and are described in details in the supporting information (Figures

S6 and S7). This work also demonstrates the accuracy of measurements. For this reason, 5 runs were performed at each temperature for one sample to obtain average Stribeck curves. Balls and plates were changed between every samples to limit measurement error. The evolution of the CoF versus sliding velocity (or RPM) is divided into four domains, as shown in Figure 1. The first domain (Figure 1-1) at a low sliding velocity is called the boundary regime and shows that the CoF is influenced by the large amount of frictional force provided by the substrate. Then at higher sliding velocity, a second domain appears (Figure 1-2) in which the normal force from the specimen began to spread the plates and ball leading to a pronounced decrease of the CoF; however, some frictional forces from the substrate still remain. This second domain is called a mixed regime. The third domain (Figure 1-3) is called the elasto-hydrodynamic domain and presents a minimum of CoF. In the last domain (Figure 1-4) an increase in the CoF, caused by an increase in the film thickness of the sample, is observed. This is the hydrodynamic behavior of the specimen.

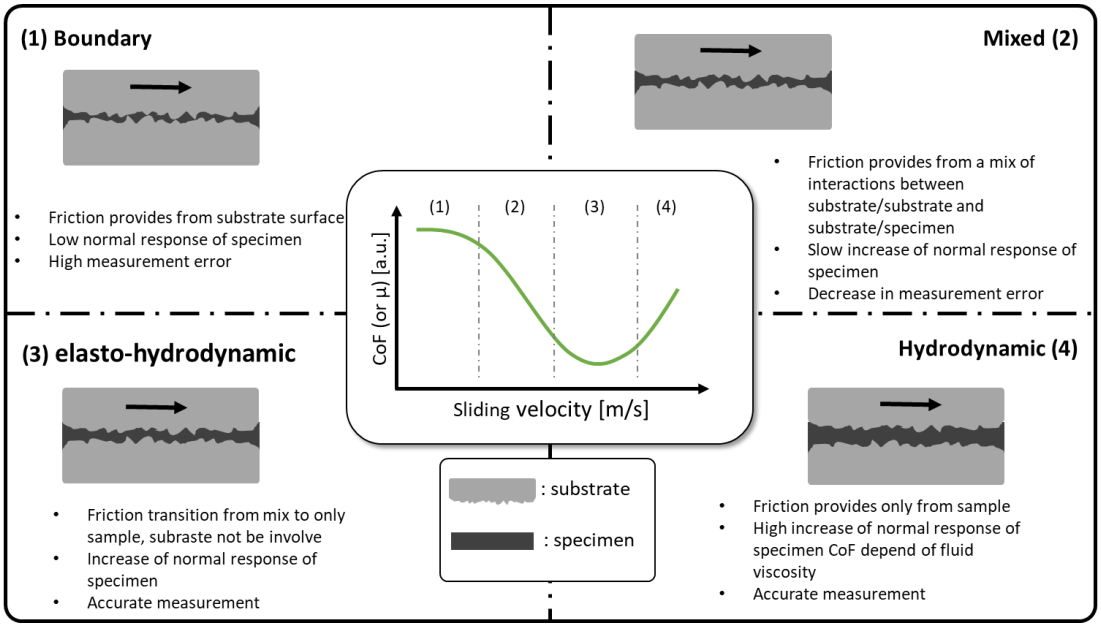

Figure 1: Schematic overview of the Stribeck curve and all different domains with (1) boundary (2) mixed (3) elasto-hydrodynamic and (4) hydrodynamic ones

3 Results and discussion:

This work is based on two reference asphalt samples with nearly the same high-temperature viscosity, penetration grade, and crystallizable fraction content. The crystallizable fractions were determined by differential scanning calorimetry (Figures S8 and S9) and differ by only 1% in weight, and therefore is considered as non-influencing. The major differences between asphalts A and B were the sources and asphaltene content (gap of ≃10wt%). These two asphalt samples allow a comparison of the influence of asphaltene content before and after aging and its influence on the coefficient of friction for the same asphalt penetration grade (35/50) (Table S2).

The first set of analyses investigated the influence of short- and long-term laboratory aging on the penetration grade, ring and ball temperature, asphaltene content, and aging index using FTIR. Table shows all the results that characterize asphalt aging and its physical-chemical evolution. These tests revealed that there was a gradual increase in the asphaltene content (+47% for asphalt A and +125% for asphalt B), in ring and ball temperature (RBT) (+40% for asphalt A and +35% for asphalt B), and a decrease in the penetration grade (-70% for asphalt A and -58% for asphalt B) after RTFOT + PAV for 40h. There were similarities between specimens A and B in terms of the evolution of the penetration grade (Figure S10). However, differences were observed in the RBT and asphaltene content. The asphaltene generated by the thermal oxidative process causes the global hardening of the asphalt binder and generally results to the creation of new asphaltene molecules known as oxidized asphaltenes.

The next part investigates the influence of these types of thermal modifications on the tribological behavior of asphalts. Tribological analysis of aged samples were performed at different temperatures to investigate the influence of these treatments on the evolution of the Coefficient of Friction (CoF) with sliding velocity.

Figure 2 shows the results of the tribological analysis performed on asphalt A before and after short- and long-term aging. Four domains of the Stribeck curve were observed for all temperatures, except at 120°C where the hydrodynamic domain is not yet reached in the sliding velocity range investigated and where all samples show similar behavior. The absence of this domain is related to the low viscosity and the Newtonian behavior in a wide range of shear rate of the asphalt at this temperature. The friction between two plates still exist at high sliding velocity which can explain high measurement error. When the temperature decreases, all domains shift to smallest sliding velocity, and the hydrodynamic behavior of the specimen becomes more and more pronounced. An increase of the CoF in this domain is related to an increase of the film thickness, indirectly observed by the gap evolution (Figures S11-14). As the film thickness increases for a given sliding velocity, the shear rate decreases ($\dot{\gamma} \propto \frac{1}{h}$).

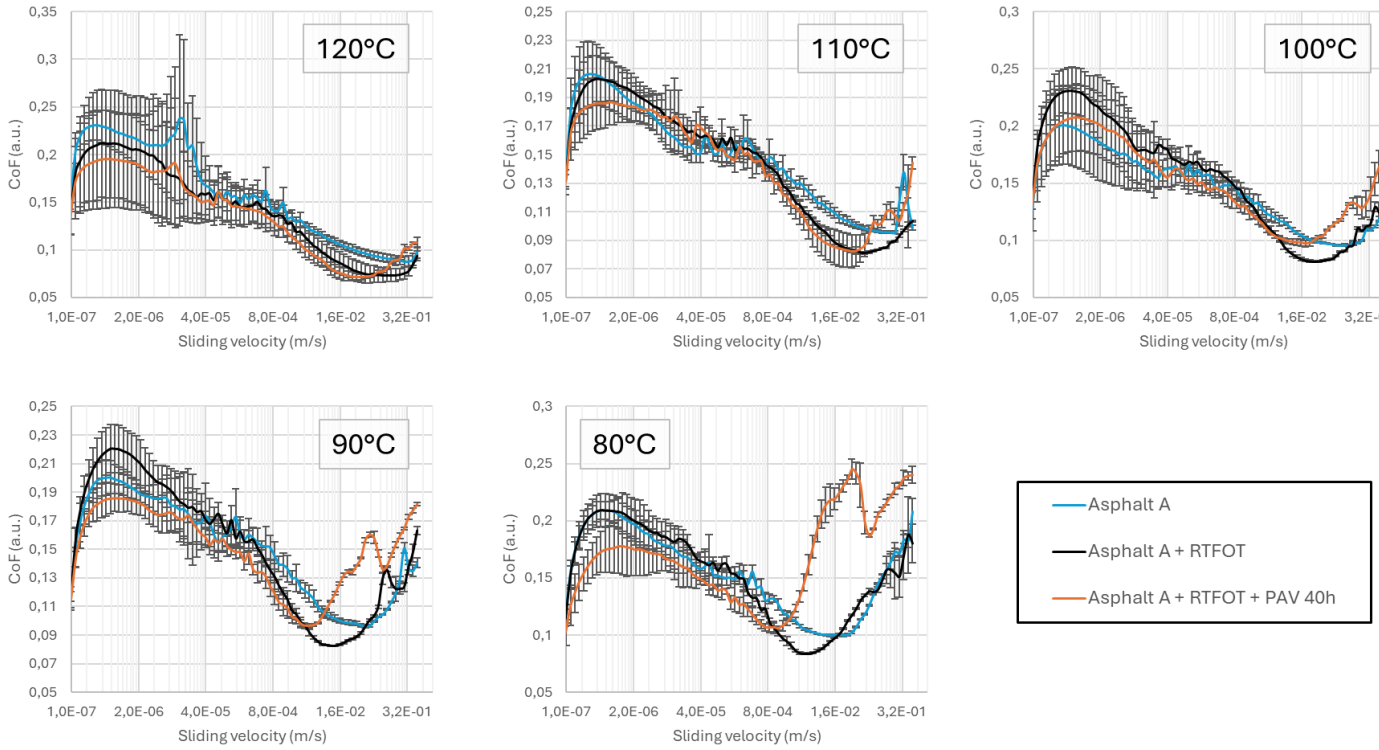

Figure 2: Stribeck curves of reference asphalt A in blue, after RTFOT in black and after RTFOT + PAV 40h in orange at 120, 110, 100, 90 and 80°C

An increase in asphalt viscosity may cause the increase of the coefficient of friction in hydrodynamic domain. The shear rate in tribological analysis can be estimated over 1000 s^{-1}, and the probability of

observing a nonlinear behavior is high, as shown in Eyssautier J. al. works[37], where the shear thinning behavior of crude oil appears at 80°C with a shear rate of 100 s^{-1}.

The minimal friction coefficient obtained on the Stribeck curves at the different temperatures studied are presented in Figure 3 for all asphalt A type samples. These results reveal that there was a gradual increase in the minimal coefficient of friction when the temperature decreased after aging. Reference asphalt shows a low influence of temperature on minimal coefficient of friction as compared to other works[26,27]. But frictional coefficient cannot be resume to minimal coefficient of friction. The coefficient of friction of this sample in the hydrodynamic domain increases for all samples when the temperature decreases. As previously discussed, the asphalt material can show a non-Newtonian behavior and this phenomenon, related to the normal response of the sample, induces the appearance of the hydrodynamic behavior. The increase in the minimal CoF was caused by a reduction in the mixed domain, which was governed by the coexistence of friction from susbtrate / substrate and substrate / asphalt. The influence of the asphalt specimen appeared at lower sliding velocity. This was observed for all the aged and non-aged asphalts. It is interesting to note that higher minimal friction coefficient is obtained for asphalt A aged with RTFOT + PAV process at 80°C.

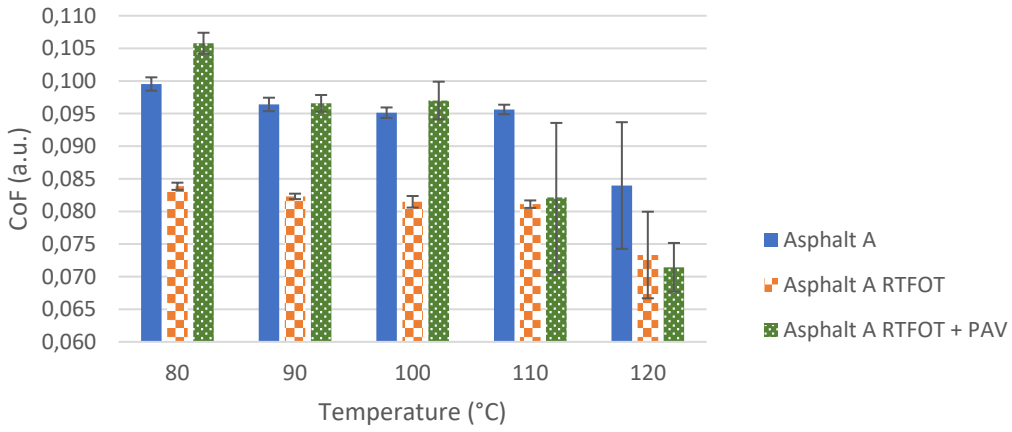

Figure 3: Comparison between minimal CoFs obtained with asphalt A in blue, after RTFOT in orange and after RTFOT + PAV 40h in green at 120, 110, 100, 90 and 80°C

Short- and long-term aging exhibit similar behavior with respect to a shift of all Stribeck domains at lower sliding velocities (Figure 2). Mixed and boundary regimes were usually less used because of the

high measurement error. However, these treatments have different effects on elasto-hydrodynamic and hydrodynamic domains.

For Asphalt A, Rolling Thin Film Oven Test aging induces a decrease in the coefficient of friction in the elasto-hydrodynamic domain and maintains a similar behavior in the hydrodynamic regime compared to the reference asphalt. The first observation can be explained by the oxidation of asphalt, which leads to an increase in the sulfoxide index, which differs from natural asphaltene. Lee et al.[38] shows four different effects of nanoparticles on lubricating properties with rolling, mending and polishing effects and generation of protective film. Another work[25] deals with the incorporation of graphene nanoparticles in asphalt and explained the decrease in the coefficient of friction by the mending effect. For asphalt A after RTFOT, a possible hypothesis consists of the generation of a new nanoaggregate of oxidized asphaltene, which can help lubrication by one of these different effects.

RTFOT + Pressure Aging Vessel (40h) induces an increase of the minimum coefficient of friction in the elasto-hydrodynamic and hydrodynamic Stribeck domains due to the increase in asphaltene content. In relation to the previous hypothesis dealing with mending effect, in this case, it was possible to identify a limit concerning nanoparticles content to improve the lubrication properties. These limits were reached with this laboratory aging and asphalt.

The same general trend is obtained with asphalt B for long-term aging samples Figure 4. All Stribeck domains were identified at temperatures ranging from 110 °C to 80°C. A shift in all Stribeck domains at lower sliding velocities and an increase in the coefficient of friction in the hydrodynamic domain is observed as for Asphalt A. Regarding the elasto-hydrodynamic and mixed domains of long-term aging asphalt B, the CoF was lower than that obtained for reference asphalt B at each temperature tested.

Short-term aging sample B presents a more complex modification of the coefficient of friction. It was always higher in all the domains and the results were reproductible. In this case, short-term aging appears to have an important influence on the lubricity ability of the binders, which is difficult to

explain. However, the needle penetration results are similar to those of asphalt A and the behavior of this asphalt after long term aging was more coherent as compared to asphalt A.

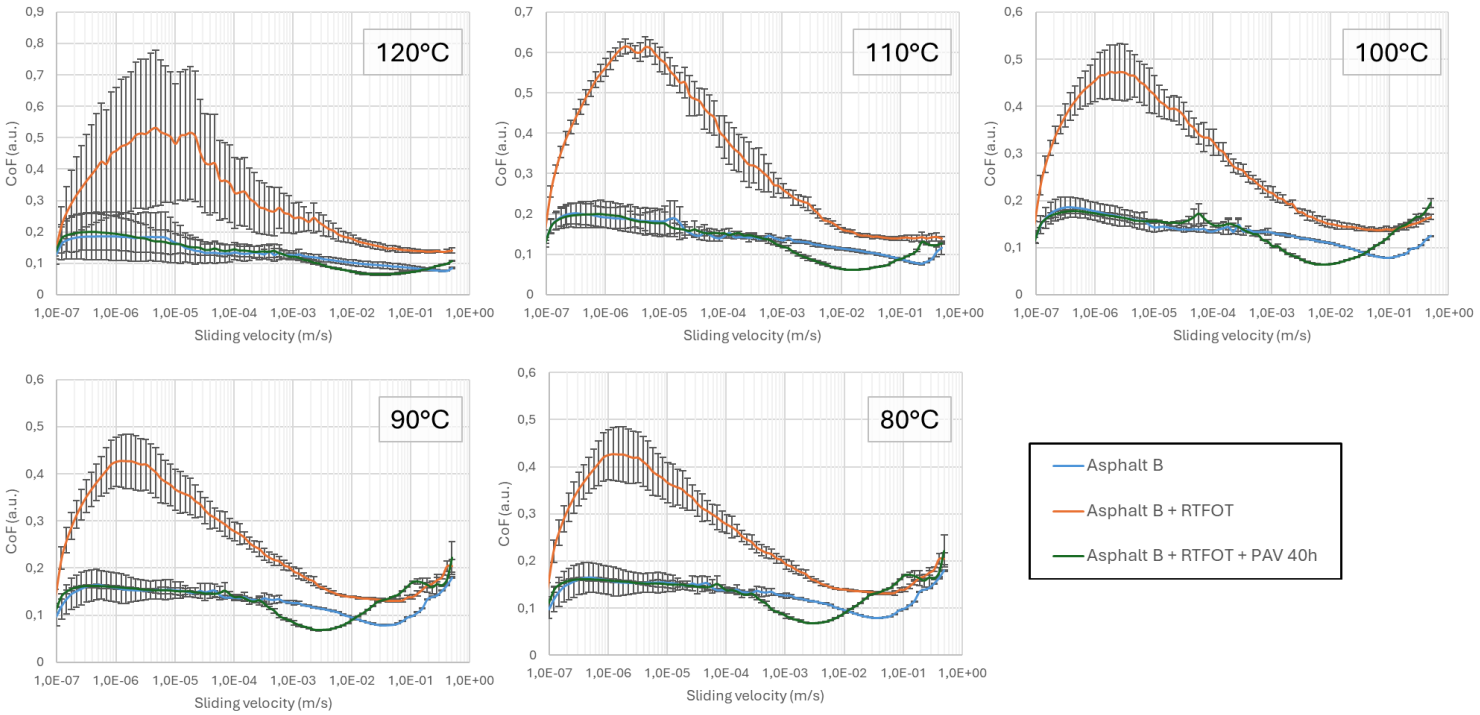

Figure 4: Stribeck curves of reference asphalt B in blue, after RTFOT in orange and after RTFOT + PAV40h in green at 120, 110, 100, 90 and 80°C

The minimal coefficients of friction for all the asphalt B samples are compared in Figure 5. The same behavior was observed as a function of temperature for asphalt B reference (i.e. unaged) and the long-term aging. The minimal CoF slightly increased with the decrease of temperature. In the case of Rolling Thin Film Oven Test treatment (short-term aging) a different behavior from that of asphalt A with the same aging state was observed. The CoF decreases slightly with the decrease in temperature only for this sample and the influence of temperature is difficult to explain again.

These aging processes show that it is difficult to compare different samples using only the minimal coefficient of friction obtained from the elasto-hydrodynamic domain.

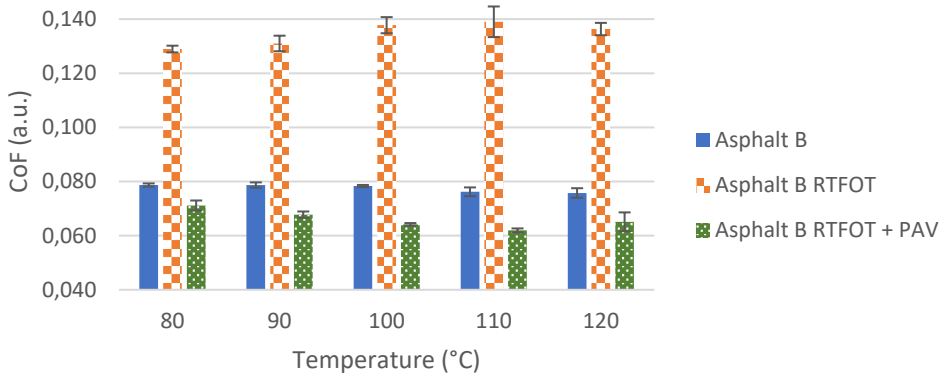

Figure 5: Comparison between minimal CoFs obtained with asphalt B in blue, after RTFOT in orange and after RTFOT + PAV 40h in green at 120, 110, 100, 90 and 80°C

To summarize, some similarities were observed after thermal oxidative aging. The hydrodynamic domain occurred at the smallest sliding velocity and was more pronounced for the two asphalts tested after RTFOT + Pressure Aging Vessel for 40h. This behavior may be related to the increase in viscosity and the elastic behavior of asphalt in hydrodynamic domain which induces an increase of the normal response (i.e. increase the film thickness) of the asphalt at each temperature investigated. A final comment concerns the influence of asphaltene on the coefficient of friction in elasto-hydrodynamic and hydrodynamic domains; asphalt A has twice as much asphaltene as asphalt B and presents a higher coefficient of friction.

To confront laboratory aging and natural aging processes, the results obtained with the Rolling Thin Film Oven Test + Pressure Aging Vessel treatment on asphalts A and B were compared to the results obtained for asphalt extracted from the Reclaimed Asphalt Pavement (different from asphalt A and B), which was naturally aged. This comparison was realized for information purposes only because no link exists between asphalt A, B, and asphalt from RAP, and the information cannot be generalized to every asphalt. The complete Stribeck curves are shown in Figure 6. It is important to keep in mind that the origin and aging history of this RAP extract are unknown; however, the behavior of this asphalt seems

to be similar to that of asphalt A and less lubricating than asphalt B. In terms of asphaltene content, penetration grade, Ring and Ball Temperature, and Infra-Red oxidative index, asphalt A and RAP extract have some similarities (Table 1). This may explain the close behavior in the elasto-hydrodynamic and hydrodynamic domains. However, boundary and mixed domains presented higher coefficients of friction for the extracted asphalt, particularly at 110 °C and 100°C. However, the oxidation indices presented in Table 1 are slightly higher for A_{RAP} than for $AA_{RTFOTPAV}$ [I_{CO} (A_{RAP}) = 8,0 I_{CO} ($AA_{RTFOTPAV}$) = 6,7 I_{SO} (A_{RAP}) = 22,6 I_{SO} ($AA_{RTFOTPAV}$) = 19,2]. This difference in the oxidation state of asphalt from RAP originates from ultraviolet radiation, and water exposure which were not simulated in laboratory treatments. This radiation oxidation provides asphalt with higher viscosity (Table 1 and Figure S3) and may explain higher coefficient of friction in almost all Stribeck domains.

It was observed that aging induces an increase in asphaltene content which seems to influence lubricant behavior of asphalt. In this part, the effect of asphaltene content on the coefficient of friction

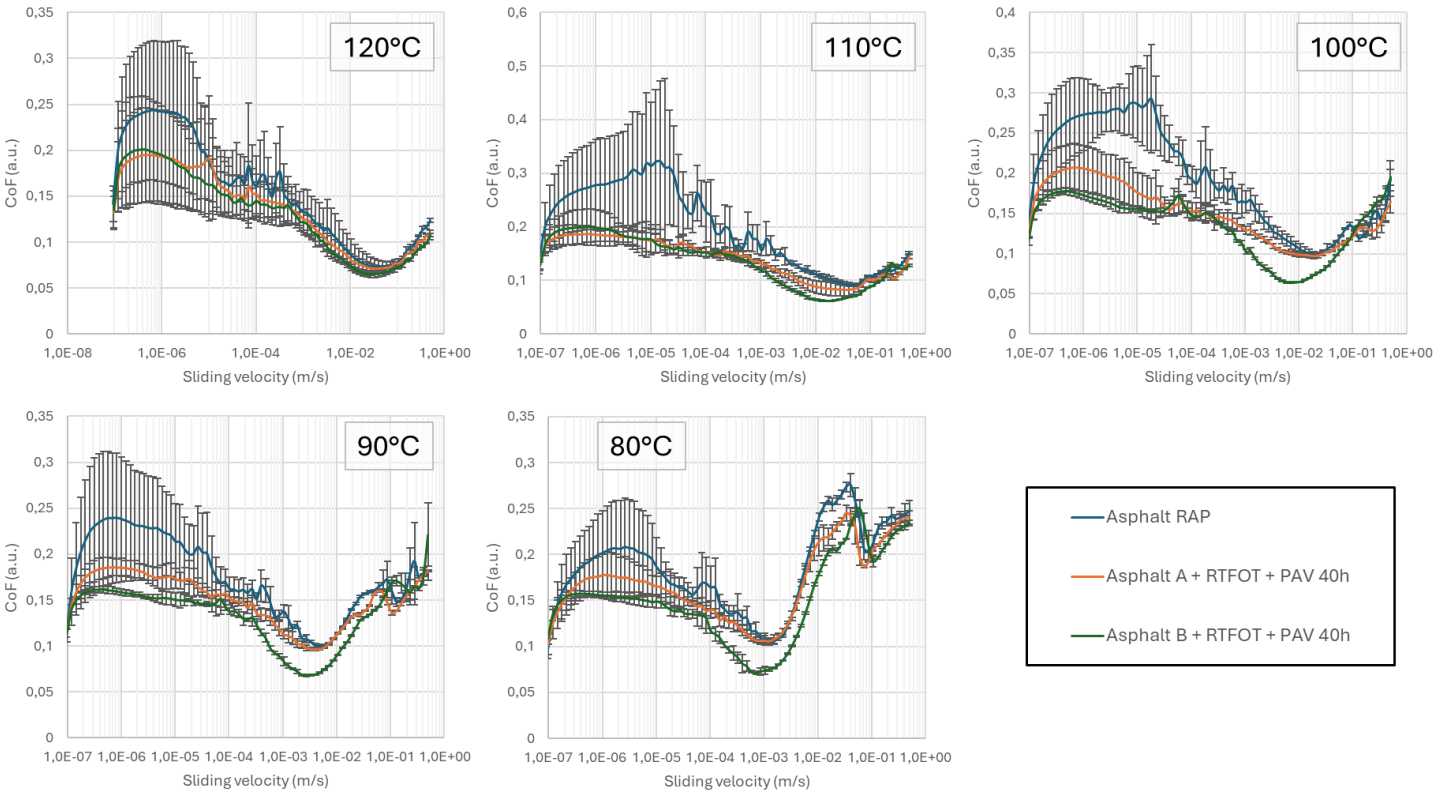

Figure 6: Comparison between asphalt sample A and B after RTFOT + PAV40h respectively in orange and green and asphalt extract from RAP in blue at 120, 110, 100, 90 and 80°C

is investigated based on a model system with controlled asphaltene content. Oxidized asphaltenes are not considered to simplify the comprehension of these complex materials.

Systems with controlled asphaltene contents were first prepared. Samples with 0 (i.e., 100% maltene), 15 and 20.3 wt% of asphaltene were prepared for asphalt A. These specimens were analyzed using the same experimental protocol, and the results are shown in Figure 7. Maltene, without N-heptane extracted asphaltene, shows only the three first domain of the Stribeck curve expected at 80°C where hydrodynamic regime appears. The other specimens presented all Stribeck domains, except at 120°C, where the sample viscosity induced by the lower asphaltene content was probably too weak to generate a hydrodynamic pressure in the velocity range investigated. These results indicate that an increase in asphaltene content modifies the elasto-hydrodynamic, hydrodynamic regimes[39] and viscosity[37,40]. In these two domains, an increase of the asphaltene content generates an increase in the coefficient of friction due to increased interaction between the particles. This probably generates higher values of the first normal stress difference, implying an increase of the normal force generated from the asphalt sample on the rheometer axis. In comparison, the boundary and mixed regimes are not significantly affected.

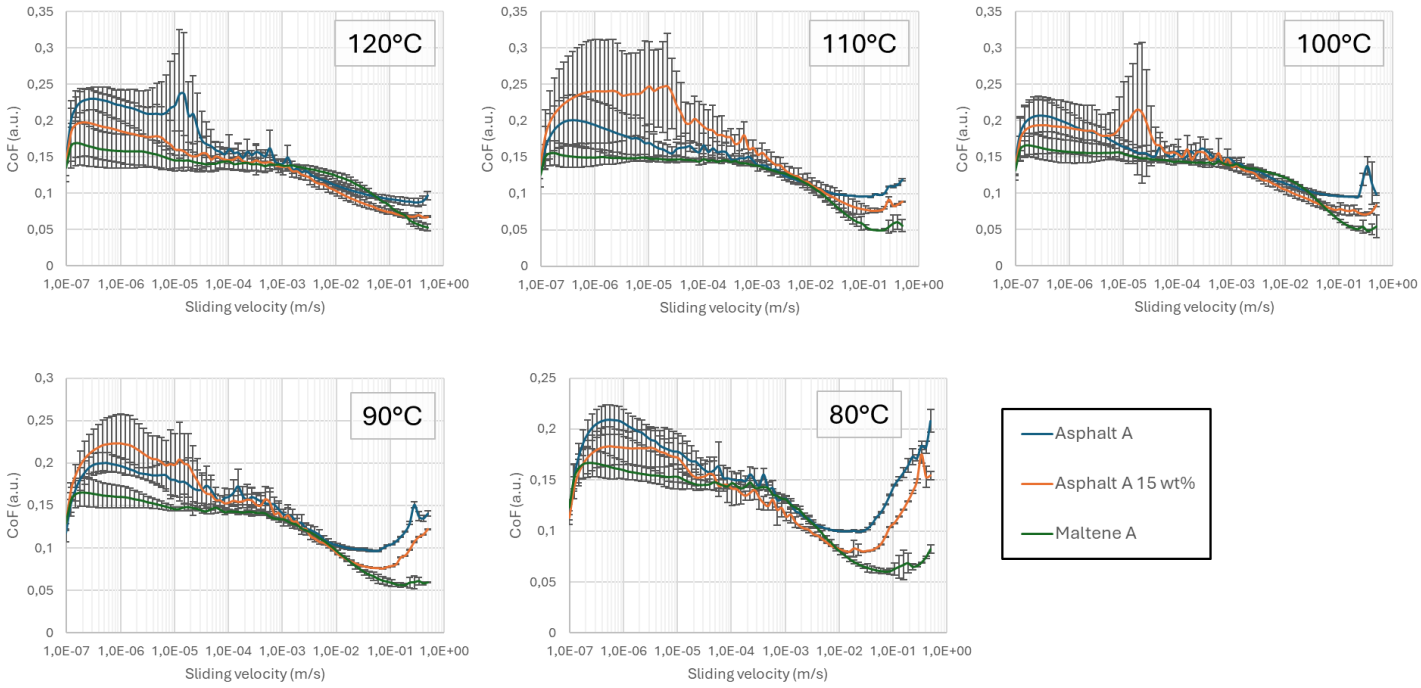

Figure 7: Stribeck curves of modified asphalt A reference asphalt at 20wt% in blue, asphalt A orange with 15 wt% of asphaltene in orange and maltene A in green at 120, 110, 100, 90 and 80°C

287

288 Similar experiments were performed on asphalt B to obtain two different asphaltene contents (11.4
289 and 15.0 wt%) and results are shown Figure 8. All Stribeck domains appeared at all investigated
290 temperatures. As a result, the influence of asphaltene content was highlighted. For asphalt B, the
291 mixed, elasto-hydrodynamic, and hydrodynamic regimes were modified. An increase of the asphaltene
292 content induces a higher CoF in all domains and a shift of these regimes at lower sliding velocities. As
293 seen in the previous part of this study, asphalt B appears to be more sensitive to asphaltene variation
294 as the oxidation state varies.

295 These results show that samples with different origins and similar viscosities, RBT, and penetration
296 grades (Table 1) can evolve differently.

297

298

299

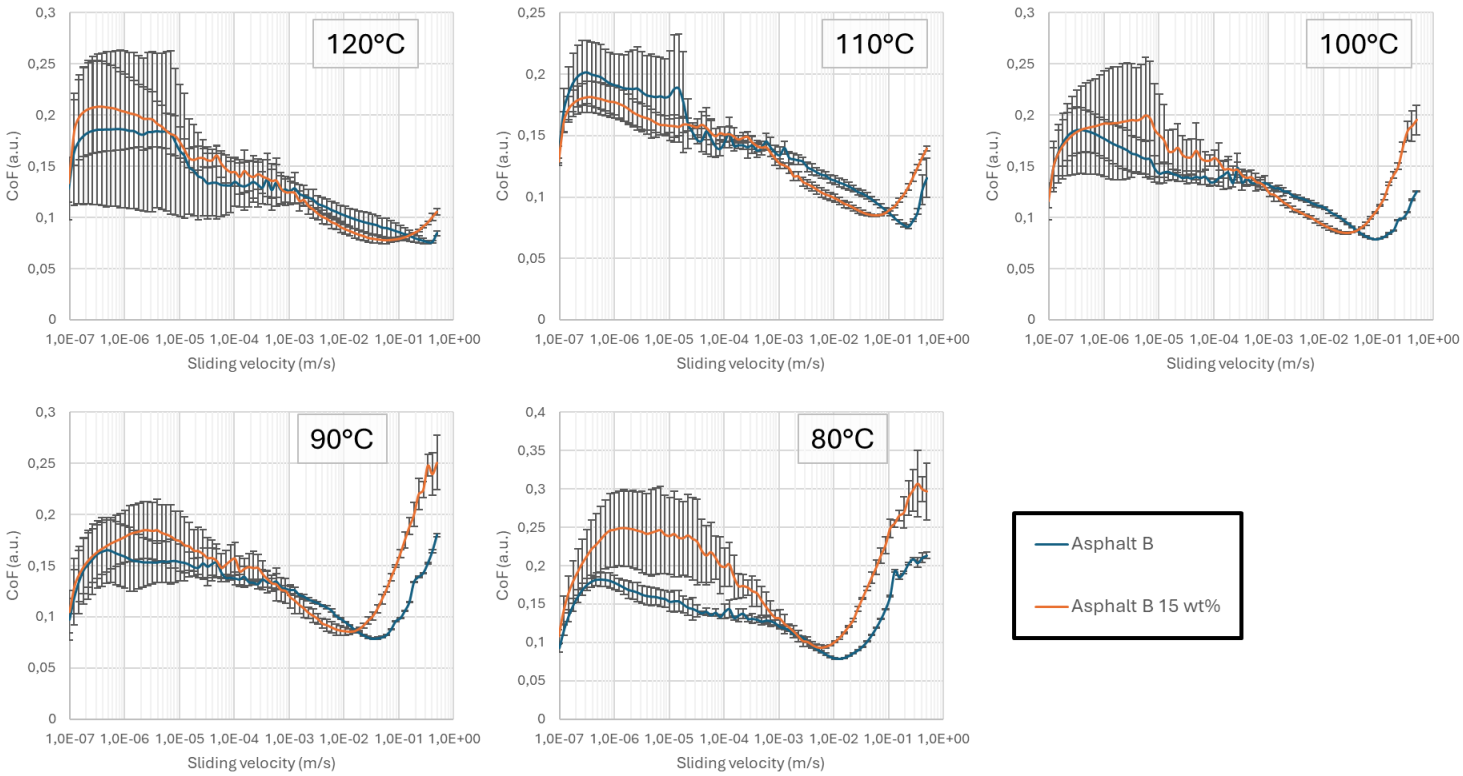

Figure 8: Stribeck curves of modified asphalt B reference asphalt at 10wt% in blue, asphalt A orange with 15 wt% of asphaltene in orange at 120, 110, 100, 90 and 80°C

The asphaltene content parameter can explain the shift of the four Stribeck domains at lower sliding velocities when it increases. For the modified asphalts presented in this section, the results show a trend when the asphaltene content increases, the minimal coefficient of friction also increases. However, for aged samples, this hypothesis cannot be applied. Nevertheless, the influence of the asphaltene content on the CoF in the hydrodynamic regime was similar for model and aged asphalts. The peptization of asphaltene (i.e. the amount of resin fraction), polarity of asphaltenes, and the initial aggregation state of asphaltenes may explain the differences between the model and aging methods.

4 Conclusion:

The aim of the present study was to examine the influence of natural aging of asphalt coming from reclaimed asphalt pavement and the effect of laboratory thermal aging of asphalts (RTFOT and PAV) on lubrication properties. The variation of the asphaltene content that occurs during the aging process

312 is the key parameter that governs tribological properties and were specifically studied using model
313 asphalts with controlled asphaltene content.

314 After short- and long-term laboratory aging, asphalts showed physical hardening induced by oxidative
315 reaction which generated an increase in ring and ball temperature, oxidative indices and asphaltene
316 content and a decrease in the needle penetrability. An increase of the asphaltene content increased
317 the viscosity at high temperature. Those observations agree with literature data.

318 The Rolling Thin Film Oven test of asphalts with a penetration grade of 35/50 showed different
319 behaviors depending on the origin of the asphalt. Generation of low quantity of oxidized asphaltene
320 could modify the lubricity ability of the asphalts both negatively and positively. In general, short-term
321 aging slightly modifies the coefficient of friction in elasto-hydrodynamic and hydrodynamic domains.
322 After long-term aging (RTFOT + Pressure Aging Vessel for 40h), the asphalt binders behaviors were
323 modified by a shift of all Stribeck domains at the smallest sliding velocities and a slight variation of the
324 minimal coefficient of friction (CoF). The CoF in hydrodynamic domains sharply increased, due to the
325 increase in asphaltene content, which induced a higher hydrodynamic pressure.

326 In general, asphalt aging induced an increase in viscosity and a similar effect can be observed in the
327 lubricity ability of asphalts in a hydrodynamic domain which comes from an increase of the coefficient
328 of friction. The model system analysis confirms the influence of asphaltene in the hydrodynamic
329 domain. Higher asphaltene content degrades the lubricity ability induced by an increase of particles
330 interactions. Asphalt lubricity, in addition to the viscosity parameter, can explain a part of asphalt
331 concrete workability issues when reclaimed asphalt pavement is used in the composition of a road.

332 This work extends collected data on asphalt samples from different sources with aging treatment. It
333 also demonstrates the efficiency of tribological analysis as a complementary tool to viscosity
334 measurement in order to investigate asphalt formulations composed of reclaimed asphalt pavement.
335 More experiments are still necessary to confirm and expend these general hypotheses to other
336 asphalts from different origins.

5 References:

1. Sala B. *Route de France - Etat de la route - 2022.* https://www.routesdefrance.com/etat-de-la-route-2022-6668/. 2022:1-28

2. Jewell DM, Albaugh EW, Davis BE, Ruberto RG. Integration of Chromatographic and Spectroscopic Techniques for the Characterization of Residual Oils. *Ind Eng Chem Fund*. 1974;13(3):278-282. doi:10.1021/i160051a022

3. Kharrat AM, Zacharia J, Cherian VJ, Anyatonwu A. Issues with Comparing SARA Methodologies. *Energy Fuels*. 2007;21(6):3618-3621. doi:10.1021/ef700393a

4. Lesueur D. The colloidal structure of bitumen: Consequences on the rheology and on the mechanisms of bitumen modification. *Advances in Colloid and Interface Science*. 2009;145(1-2):42-82. doi:10.1016/j.cis.2008.08.011

5. Pfeiffer JPh, Saal RNJ. Asphaltic Bitumen as Colloid System. *J Phys Chem*. 1940;44(2):139-149. doi:10.1021/j150398a001

6. Madeira NCL, Lacerda V, Romão W. Characterization of Asphalt Aging by Analytical Techniques: A Review on Progress and Perspectives. *Energy Fuels*. 2022;36(11):5531-5549. doi:10.1021/acs.energyfuels.2c00446

7. Ferrotti G, Baaj H, Besamusca J, et al. Comparison between bitumen aged in laboratory and recovered from HMA and WMA lab mixtures. *Mater Struct*. 2018;51(6):150. doi:10.1617/s11527-018-1270-4

8. Hofko B, Cannone Falchetto A, Grenfell J, et al. Effect of short-term ageing temperature on bitumen properties. *Road Materials and Pavement Design*. 2017;18(sup2):108-117. doi:10.1080/14680629.2017.1304268

9. Hu Y, Si W, Kang X, et al. State of the art: Multiscale evaluation of bitumen ageing behaviour. *Fuel*. 2022;326:125045. doi:10.1016/j.fuel.2022.125045

10. Siddiqui MN, Ali MF. Studies on the aging behavior of the Arabian asphalts. *Fuel*. 1999;78(9):1005-1015. doi:10.1016/S0016-2361(99)00018-6

11. NF EN 12607-1 Bitumes et liants bitumineux Détermination de la résistance au durcissement sous l'effet de la chaleur et de l'air — Partie 1 : Méthode RTFOT, 2007.

12. NF EN 14769 : Bitumes et liants bitmineux - Vieillissement long-terme accéléré réalisé dans un récipient de vieillissement sous pression (PAV). Published online 2013.

13. Li J, Xing X, Hou X, Wang T, Wang J, Xiao F. Determination of SARA fractions in asphalts by mid-infrared spectroscopy and multivariate calibration. *Measurement*. 2022;198:111361. doi:10.1016/j.measurement.2022.111361

14. Petersen JC. Chemical composition of asphalt as related to asphalt durability. Published online 1984. doi:https://doi.org/10.1016/S0376-7361(09)70285-7

15. Woydt M, Wäsche R. The history of the Stribeck curve and ball bearing steels: The role of Adolf Martens. *Wear*. 2010;268(11-12):1542-1546. doi:10.1016/j.wear.2010.02.015

16. Canestrari F, Ingrassia LP, Ferrotti G, Lu X. State of the art of tribological tests for bituminous binders. *Construction and Building Materials*. 2017;157:718-728. doi:10.1016/j.conbuildmat.2017.09.121

17. Baumgardner GL, Reinke GR. Lubricity Properties of Asphalt Binders Used in Hot-Mix and Warm-Mix Asphalt Pavements. Published online 2012.

18. Reinke G, Baumgardner GL, Engber SL. Warm mix asphalt binder compositions containing lubricating additives. Published online March 24, 2014.

19. Bairgi BK, Manna UA, Tarefder RA. Tribological Evaluation of Asphalt Binder with Chemical Warm-Mix Additives. In: *Airfield and Highway Pavements 2019*. American Society of Civil Engineers; 2019:266-273. doi:10.1061/9780784482469.027

20. Bairgi BK, Mannan UA, Tarefder RA. Tribological Evaluation for an In-Depth Understanding of Improved Workability of Foamed Asphalt. *Transportation Research Record*. 2019;2673(4):533-545. doi:10.1177/0361198119835510

21. Bairgi BK, Mannan UA, Tarefder RA. Tribological Approach to Demonstrate Workability of Foamed Warm-Mix Asphalt. *J Mater Civ Eng*. 2019;31(9):04019191. doi:10.1061/(ASCE)MT.1943-5533.0002843

22. Bairgi BK, Mannan UA. Influence of foaming on tribological and rheological characteristics of foamed asphalt. *Construction and Building Materials*. 2019;205:186-195. doi:10.1016/j.conbuildmat.2019.02.009

23. Bairgi BK, Tarefder RA. Effect of Foaming Water Contents on High-Temperature Rheological Characteristics of Foamed Asphalt Binder. In: *International Conference on Transportation and Development 2018*. American Society of Civil Engineers; 2018:243-251. doi:10.1061/9780784481554.025

24. Bairgi BK, Tarefder RA. Characterization of foaming attributes to binder tribology and rheology to better understand the mechanistic behavior of foamed asphalt. *Int J Pavement Res Technol*. 2021;14(1):13-22. doi:10.1007/s42947-020-0283-x

25. Yan T, Ingrassia LP, Kumar R, et al. Evaluation of Graphite Nanoplatelets Influence on the Lubrication Properties of Asphalt Binders. *Materials*. 2020;13(3):772. doi:10.3390/ma13030772

26. Ingrassia LP, Lu X, Marasteanu M, Canestrari F. Tribological Characterization of Graphene Nano-Platelet (GNP) Bituminous Binders. In: *Airfield and Highway Pavements 2019*. American Society of Civil Engineers; 2019:96-105. doi:10.1061/9780784482476.011

27. Ingrassia LP, Lu X, Canestrari F, Ferrotti G. Tribological characterization of bituminous binders with Warm Mix Asphalt additives. *Construction and Building Materials*. 2018;172:309-318. doi:10.1016/j.conbuildmat.2018.03.275

28. Mannan UA, Tarefder RA. Tribological and rheological characterisation of asphalt binders at different temperatures. *Road Materials and Pavement Design*. 2018;19(2):445-452. doi:10.1080/14680629.2016.1251961

29. Hanz AJ, Faheem A, Mahmoud E, Bahia HU. Measuring Effects of Warm-Mix Additives: Use of Newly Developed Asphalt Binder Lubricity Test for the Dynamic Shear Rheometer. *Transportation Research Record*. 2010;2180(1):85-92. doi:10.3141/2180-10

30. Wagh VP, Saboo N, Gupta A. Using tribological approach to assess production temperatures of asphalt binders. *Construction and Building Materials*. 2024;419:135513. doi:10.1016/j.conbuildmat.2024.135513

31. Jiang J, Xu D, Yu S, Ni F. Micro-structural characterization of the lubrication behavior of asphalt binder during the compaction of asphalt mixture. *Tribology International*. 2023;189:108953. doi:10.1016/j.triboint.2023.108953

32. Zhan Y, Wu H, Song W, Xu Z. Determining meso-parameters of hot mix asphalt with reclaimed asphalt pavement based on workability. *Construction and Building Materials*. 2022;359:129512. doi:10.1016/j.conbuildmat.2022.129512

33. NF EN 1427 : Bitumes et liants bitumineux - Détermination du point de ramollissement - Méthode bille et Anneau. Published online 2018.

34. NF EN 1426 : Bitumes et liants bitumineux - Détermination de la pénétrabilité à l'aiguille. Published online 2018.

35. NF EN 13302 : Bitumes et liants bitumineux - Détermination de la viscosité dynamique des liants bitumineux à l'aide d'un viscosimètre tournant. Published online 2018.

36. NF EN 12607-1 : Bitumes et liants bitumineux - Détermination de la résistance au durcissement sous l'effet de la chaleur et de l'air. Published online 2014.

37. Eyssautier J, Hénaut I, Levitz P, Espinat D, Barré L. Organization of Asphaltenes in a Vacuum Residue: A Small-Angle X-ray Scattering (SAXS)–Viscosity Approach at High Temperatures. *Energy Fuels*. 2012;26(5):2696-2704. doi:10.1021/ef201412j

38. Lee K, Hwang Y, Cheong S, et al. Understanding the Role of Nanoparticles in Nano-oil Lubrication. *Tribol Lett*. 2009;35(2):127-131. doi:10.1007/s11249-009-9441-7

39. Solomon SE, Doubleday P, Landry J, John VT, Pesika NS. Lubrication mechanisms of dispersed carbon microspheres in boundary through hydrodynamic lubrication regimes. *Journal of Colloid and Interface Science*. 2023;650:1801-1810. doi:10.1016/j.jcis.2023.07.089

40. Luo P, Gu Y. Effects of asphaltene content on the heavy oil viscosity at different temperatures. *Fuel*. 2007;86(7-8):1069-1078. doi:10.1016/j.fuel.2006.10.017